

Improving PCM Melting Performance using Asymmetric Fin Designs in Rectangular Enclosures

Fatima Zohra Mecieb

Laboratory of Reactive Systems and Materials, Djillali Liabes University, Sidi Bel Abbes, Algeria
fatima.mecieb@univ-sba.dz (corresponding author)

Samir Laouedj

Laboratory of Reactive Systems and Materials, Djillali Liabes University. Sidi Bel Abbes, Algeria
s.laouedj@gmail.com

Received: 8 June 2024 | Revised: 18 June 2024 | Accepted: 5 July 2024

Licensed under a CC-BY 4.0 license | Copyright (c) by the authors | DOI: <https://doi.org/10.48084/etasr.8063>

ABSTRACT

This study investigates the enhancement of heat transfer in Latent Heat Thermal Energy Storage (LHTES) systems by using internal fins within a rectangular enclosure. Using lauric acid as the Phase Change Material (PCM), the impact of different fin configurations on the melting process is examined. A numerical model, incorporating the enthalpy-porosity method, is developed to simulate the phase change within the PCM. The model considers the effects of fin geometry, including variations in fin length and positioning. Results indicate that strategically placed fins significantly improve heat transfer efficiency, reducing complete melting time by more than 50% compared to a configuration of uniform-length fins. This enhancement is attributed to increased convective heat transfer facilitated by the longer fin in the lower zone of the enclosure.

Keywords-asymmetric fins; rectangular enclosures; melting enhancement; thermal energy storage

I. INTRODUCTION

Efficient thermal energy management is crucial in many industrial and domestic applications. The use of PCMs represents a promising solution for heat storage and release, thanks to their ability to absorb and release large quantities of energy as they melt and solidify [1]. However, the performance of thermal storage systems using PCMs is often limited by the low thermal conductivity of these materials. This limitation leads to irregular and slow melting and solidification, reducing the overall efficiency of thermal storage systems. To overcome this limitation, the incorporation of heat-conducting fins in PCM cavities is a commonly explored method [2]. By increasing the heat transfer surface area and promoting a more homogeneous temperature distribution, fins can significantly improve the melting rate of PCMs. The relationship between fin design in rectangular enclosures and performance, focusing on geometry parameters, and the optimization of LHTES systems has been experimentally studied [3, 4] and numerical simulations have been carried out [5, 6]. Research has explored various fin types, including straight [7, 8], inclined [9], stepped [10], and complex-form fins [11, 12], highlighting their impact on thermal performance and system efficiency. Authors in [13] reviewed theoretical studies on enhancing the melting of PCMs using fin and foam structures in TES systems. Enclosures are classified into rectangular, cylindrical, and spherical. Then the

geometric impacts of enclosures on melting behaviors are analyzed for each class. Key conclusions highlight the importance of scale analysis for simplicity and accuracy to be achieved and for the efficiency of straight fins as thermal enhancers and the complexity of non-straight fins and foam structures to be investigated. Authors in [14] evaluated the thermal performance of a finned thermal energy storage unit with nano-enhanced PCMs. Aluminum oxide nanoparticles enhance performance, which makes them ideal for energy storage applications. Authors in [15] investigated fluid flow and heat transfer in a rectangular cavity using paraffin as the PCM. By examining various aspect ratios (0.1 to 10) with a constant bottom wall temperature of 343.15 K, it was found that larger aspect ratios (≥ 1) enhanced the melting rate and natural convection, creating recirculation regions. The transition from conduction to convection-dominated heat transfer was stressed. It was shown that using a partitioned rectangular cavity with fins reduced melting time by up to 8.9% and increased temperature uniformity by up to 35%, with the best performance achieved at a 90° tilt angle [16]. Numerical analyses of a 2-D cavity with sinusoidal fins conducted in [17] revealed optimal fin configurations that significantly reduced melting and solidification times. The study identified the best periods, while in [18] the enhancement of melting in a rectangular LHTES system with a single conductive baffle was explored.

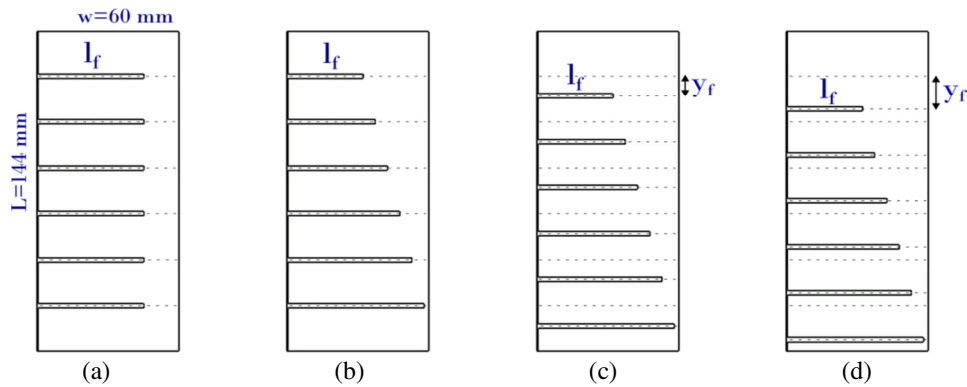


Fig. 1. Illustration of rectangular enclosure with internal fins: (a) uniform length fins (case 1), (b) symmetric stepped fins $y_f=0$ mm (case 2), (c) asymmetric stepped fins $y_f=9$ mm(case 5), (d) asymmetric stepped fins $y_f=15$ mm(case 7).

Numerical analysis revealed optimal baffle placement ($L_x/L = 0.8$) and height ($L_y/L = 0.4$) as well as improved melting rates and heat storage achieved through the enhancement of convective heat transfer.

The present study aims to extend this research by analyzing the effect of different fin configurations on PCM melting performance in a rectangular enclosure and by investigating the impact of asymmetric fin distribution on the heat storage rate and melting uniformity. Several fin configurations, including size, shape, and spatial arrangement, are explored to determine the optimal configurations for maximizing the melting rate. Numerical simulations are used to model the thermal and heat transfer processes involved and the results are compared with experimental data for validation.

TABLE I. THE OPERATIONAL PARAMETERS FOR THE TWO CATEGORIES OF LHTES SYSTEMS

	Fin length l_f (mm)	Downward shift y_f (mm)
Case 1	45	0
Case 2, 3, 4, 5, 6, 7	58/52.8/47.6/42.4/37.2/32	0, 3, 6, 9, 12, 15

TABLE II. THERMOPHYSICAL PROPERTIES OF LAURIC ACID [19]

Properties	PCM	Aluminum
Melting area [°C]	43.5/48.2	-
Density solid/liquid [kg/m ³]	940/885	2719/-
Conductivity-solid/liquid [W/m. K]	0.16/0.14	202.4/-
Specific heat-solid/liquid [J/kg. K]	2180/2390	871/-
Latente heat [J/kg]	187210	-
Kinematic viscosity (m ² /s)	6.7×10^{-6}	-

II. PHYSICAL MODEL AND BOUNDARY CONDITIONS

The study models a rectangular LHTES unit of 6 cm width and 14.4 cm height, with six internal aluminum fins of 2 mm thickness and 45 mm average length on the left isothermal wall (Figure 1). Three fin configurations were analyzed: uniform-length fins, symmetrical stepped fins, and asymmetrical stepped fins. Table I outlines the two categories of fin arrangement conditions discussed in this paper. Each

configuration was evaluated under an equal heat transfer area and heat storage capacity, with the left wall maintained at 343 K and the initial PCM temperature set at 298 K. Lauric acid was utilized as the PCM, with properties listed in Table II.

III. NUMERICAL MODEL

The enthalpy-porosity approach was employed to simulate the melting process. Key assumptions included two-dimensional, incompressible laminar flow, negligible viscous dissipation, and variable thermophysical properties. The following governing equations were solved by implementing the ANSYS FLUENT software with structured quad cells and employing the SIMPLEX algorithm for pressure-velocity coupling, while the equations of momentum and energy are discretized by the second-order upwind scheme using a time step of 0.1 s.

- Continuity:

$$\frac{\partial \rho}{\partial t} + \nabla \cdot (\rho \vec{u}) = 0 \tag{1}$$

where \vec{u} is the velocity vector and ρ is the fluid density.

- Momentum:

$$\frac{\partial}{\partial t} (\rho \vec{u}) + \nabla \cdot (\rho \vec{u} \vec{u}) = \mu \nabla^2 \vec{u} - \vec{\nabla} P + \rho \vec{g} + \vec{S} \tag{2}$$

where P is the static pressure and \vec{S} is the source term defined as:

$$\vec{S} = A_{mush} \frac{(1-\beta)^2}{(\beta^3 + \epsilon)} \vec{u}$$

where A_{mush} is a mushy zone constant. In this study it was taken equal to 3×10^6 . To prevent division by zero, ϵ is given a value of 0.001.

- Energy:

$$\frac{\partial}{\partial t} (\rho H) + \nabla \cdot (\rho \vec{u} H) = \nabla \cdot (k \nabla T) \tag{3}$$

where k is the thermal conductivity and T is the temperature.

The material's enthalpy (H) is determined through the addition of the sensible enthalpy (h) and the latent heat content (ΔH).

$$H = h + \Delta H \tag{4}$$

and:

$$h = h_{ref} + \int_{T_{ref}}^T C_p dT \tag{5}$$

with h_{ref} is the reference enthalpy, T_{ref} is the reference temperature and C_p is the specific heat.

The definition of the liquid fraction, β , is:

$$\begin{aligned} \beta &= 0 \text{ if } T < T_{solidus} \\ \beta &= 1 \text{ if } T > T_{liquidus} \\ \beta &= \frac{T - T_{solidus}}{T_{liquidus} - T_{solidus}} \text{ if } T_{solidus} < T < T_{liquidus} \end{aligned} \tag{6}$$

The latent heat content can be expressed in terms of the material's latent heat, L:

$$\Delta H = \beta \cdot L \tag{7}$$

IV. VALIDATION

Figure 2 illustrates the investigation of solution independence concerning mesh grids by analyzing the evolution of liquid fraction β . The study tested three different mesh sizes (6222, 13908, and 32748 cells). The findings indicated that a mesh size of 13908 cells yielded accurate solutions. The mushy-zone constant value significantly impacts the melting process of PCMs when employing the enthalpy-porosity method in numerical simulations. In this study, two A_{mush} values, 10^6 and 3×10^6 , were evaluated for their impact on simulation precision to be assessed. The optimal match with the experimental data [19] was found at $A_{mush} = 3 \times 10^6$, showing a satisfactory level of agreement with the experimental liquid fraction evolution during the melting process (see Figure 3).

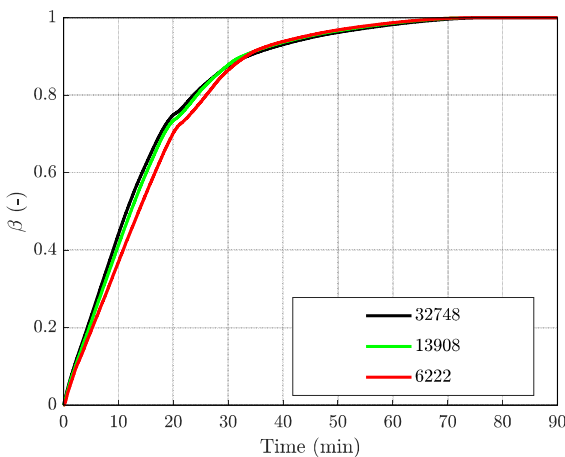


Fig. 2. Grid independence test for case 1 with uniform length fins.

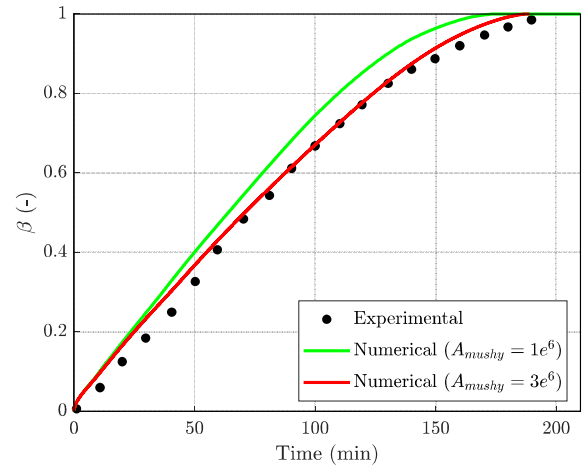


Fig. 3. Evolution of liquid fraction for two numerical mushy zone constants compared to experimental measurements [19].

V. RESULTS AND DISCUSSION

A. Melting Behavior

Figure 4 depicts liquid fraction and temperature contours for cases 1, 2, 3, 5, and 7 at different time points, providing insights into the melting progression. During the initial stages of melting ($t = 5$ min), the solid PCM adjacent to the heated wall and fins melts primarily through conduction heat transfer. The longer fin in the bottom zone increases the effective heat transfer area, facilitating more efficient conduction and accelerating the melting process in this critical region.

As the melting progresses (10 min), natural convection currents begin to develop within the liquid PCM. The buoyancy-driven flow causes the less dense liquid PCM to rise. From $t = 20$ min to 30 min, the buoyancy effect is intensified, leading to the accumulation of liquid PCM in the upper half, with a mushy zone forming along the lower wall. For $t = 40$ min, almost all the PCM has melted into the liquid state, except for small solid residues observed in cases 2, 3, and 7. Interestingly, case 5 shows an entirely liquid PCM, while the base design with uniform-length fins, case 1, still retains a significant solid fraction.

Among all the cases examined, the configuration featuring stepped fins, with the longest fin strategically positioned in the lowest zone of the enclosure (case 5, $y_f=9$ mm), demonstrates the most rapid melting progression.

This accelerated melting can be attributed to the strategic placement of the extended fin in the bottom region, which enhances natural convection currents, as the melted PCM near the bottom heats up and rises due to buoyancy, creating a convective loop that accelerates melting. Additionally, these fins distribute heat more uniformly throughout the PCM, which helps maintain a more uniform temperature distribution throughout the enclosure. Also, positioning fins near the bottom maximizes contact with solid PCM, enhancing conduction heat transfer. This mitigates the formation of stagnant regions and ensures that the heat is effectively utilized for melting the PCM across the entire volume.

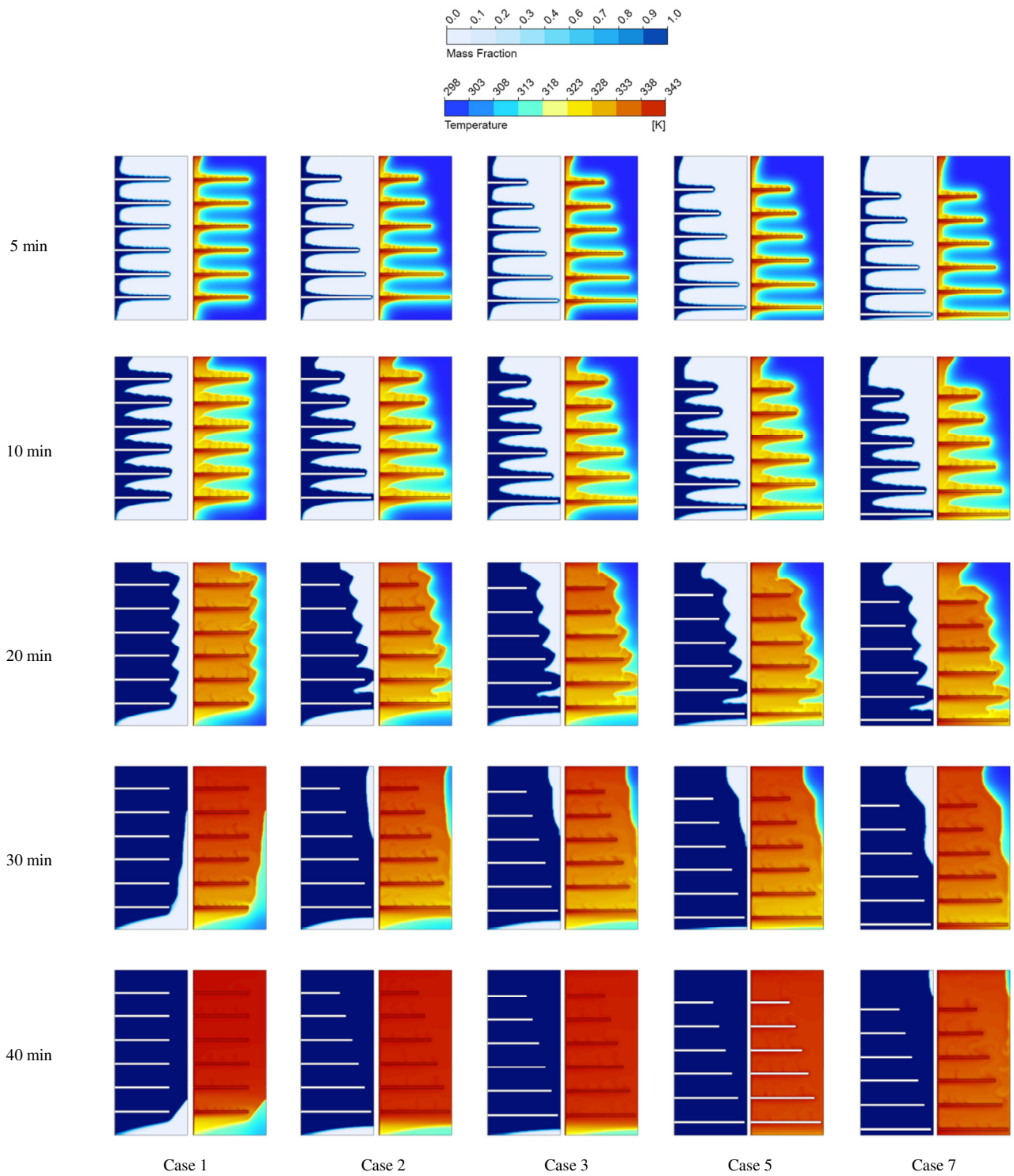


Fig. 4. Liquid fraction and temperature contours of case 1, case 2, case 3, case 5, and case 7.

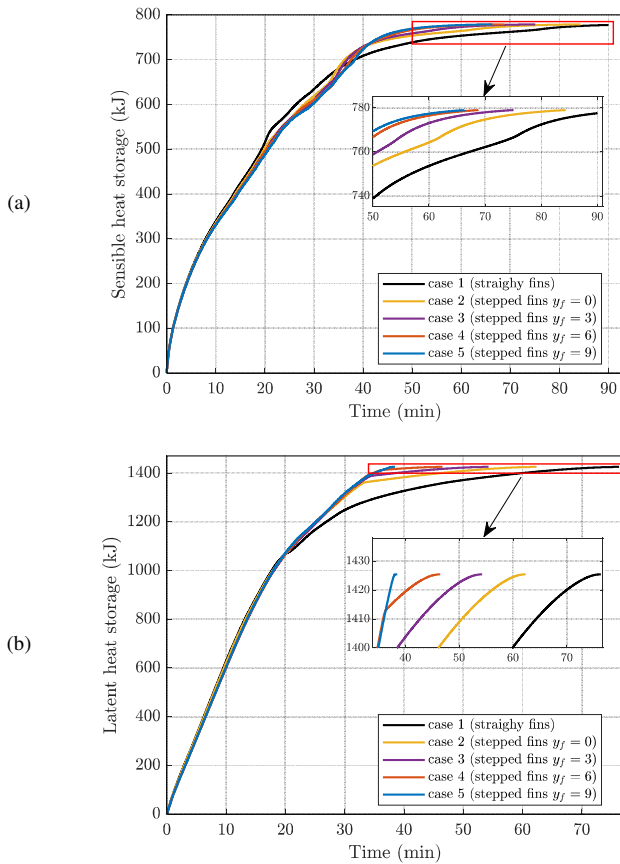


Fig. 5. Evolution of PCM: (a) sensible heat storage, (b) latent heat storage.

B. Storage Energy

Figures 5.a and 5.b display the impact of different fin configurations on sensible and latent heat storage within PCM. Uniform-length fins, case 1, show the slowest heat storage rates, while stepped fins, cases 2 to 5, demonstrate faster increases in both sensible and latent heat storage capacities. Specifically, the sensible heat storage for uniform-length fins reaches its maximum value of 777 kJ after 90 min of exposition to the heat source. In contrast, in case 5 of stepped fins with a downward shift of $y_f = 9$ mm, this value could be reached in just 59 min, which represents an improvement in sensible thermal storage efficiency of 34.44%.

For latent heat storage, uniform-length fins reach about 1336.74 kJ at 38.5 min, whereas stepped fins with a downward shift of $y_f = 9$ mm in case 5, reach approximately 1425 kJ, marking a 6.19% increase.

Over time, the differences between configurations diminish, with all approaching similar maximum values of around 780 kJ for sensible heat and 1425 kJ for latent heat.

C. Melting Time

Figure 6 depicts the relationship between the full melting time and the fin downward shift y_f . As y_f increases, there is an initial decrease in the melting time followed by a subsequent

increase. Specifically, increasing y_f from 0 to 9 mm leads to a 38 min reduction in thermal storage time. To quantify the effect of y_f on the melting heat transfer, the Melting Time Enhancement Ratio (MTER) is defined:

$$MTER = \frac{(t_{(base\ case)} - t)}{t_{(base\ case)}} \cdot 100\%$$

where t represents the full melting time for the specific case being considered. The base case used for comparison is the case with uniform-length fins.

The plot in Figure 6 indicates that MTER initially increases with increasing y_f from 0 to 15 mm, reaching a peak of 50% when $y_f = 9$ mm, case 5, and then decreases as y_f extends to 15 mm. The optimal melting improvement is observed at $y_f = 9$ mm, corresponding to case 5. Solid PCM is moved from the lower, slower-melting zone to the upper, faster-melting zone through this strategy, which effectively employs natural convection.

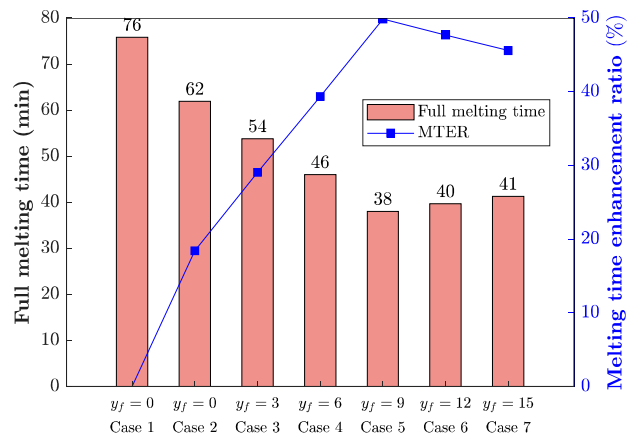


Fig. 6. Melting time for all cases.

VI. CONCLUSION

This study numerically investigated the influence of various fin configurations on the melting behavior and thermal performance of a Latent Heat Thermal Energy Storage (LHTES) system. The analysis focused on a rectangular enclosure filled with lauric acid as the Phase Change Material (PCM) and incorporated different fin arrangements, including uniform-length fins, symmetric, and asymmetric stepped fins with varying vertical displacements.

The innovative design of the asymmetric fins introduces a new approach to improving the thermal management of LHTES systems.

The results revealed that among the investigated cases, the asymmetric stepped fin arrangement with a downward shift of 9 mm, case 5, exhibited the most promising performance, reducing the total melting time by approximately 50% compared to the uniform-length fins, case 1.

The asymmetric fin configurations facilitated more efficient heat distribution and promoted natural convection currents within the melted PCM, leading to increased energy storage

rates. Specifically, case 5 achieved a 34.4% improvement in sensible heat storage efficiency and a 6.19% increase in latent heat storage compared to the uniform-length fin configuration.

The complete melting time was significantly influenced by the vertical displacement of the fins. Increasing the downward shift of the fins from 0 to 9 mm resulted in a 38 min reduction in melting time, achieving a Melting Time Enhancement Ratio (MTER) of 50%.

The significant enhancement in melting performance and heat storage efficiency achieved by the optimized asymmetric fin configuration has promising implications for various applications. This advancement can enable effective solar energy utilization and waste heat recovery in industrial settings. Additionally, buildings can be benefited from improved thermal management for heating and cooling, which can reduce energy demands. Moreover, electronic cooling systems can utilize these superior heat dissipation capabilities for enhanced performance.

The optimized asymmetric fin configuration significantly improves melting performance and heat storage efficiency, with promising implications for solar energy utilization, waste heat recovery in industries, enhanced thermal management in buildings, and superior heat dissipation in electronic cooling systems.

While the study shows that optimized fin configurations enhance LHTES performance, further research is needed into exploring different PCM materials, investigating the influence of nanoparticle enhancements, or studying the scaling effects for different enclosure sizes.

REFERENCES

- [1] F. Z. Mecieb, F. G. Bermejo, J. P. S. Fernández, and S. Laouedj, "Convective Heat Transfer During Melting in a Solar LHTES," *Engineering, Technology & Applied Science Research*, vol. 11, no. 3, pp. 7181–7186, Jun. 2021, <https://doi.org/10.48084/etasr.4165>.
- [2] H. A. Al-Salami, N. S. Dhaidan, H. H. Abbas, F. N. Al-Mousawi, and R. Z. Homod, "Review of PCM charging in latent heat thermal energy storage systems with fins," *Thermal Science and Engineering Progress*, vol. 51, Jun. 2024, Art. no. 102640, <https://doi.org/10.1016/j.tsep.2024.102640>.
- [3] B. Kamkari and D. Groulx, "Experimental investigation of melting behaviour of phase change material in finned rectangular enclosures under different inclination angles," *Experimental Thermal and Fluid Science*, vol. 97, pp. 94–108, Oct. 2018, <https://doi.org/10.1016/j.expthermflusci.2018.04.007>.
- [4] U. Temel Nazli and F. Kilinc, "Experimental investigation of variable fin length on melting performance in a rectangular enclosure containing phase change material," *International Communications in Heat and Mass Transfer*, vol. 142, Mar. 2023, <https://doi.org/10.1016/j.icheatmasstransfer.2023.106658>.
- [5] V. Safari, B. Kamkari, K. Hooman, and J. M. Khodadadi, "Sensitivity analysis of design parameters for melting process of lauric acid in the vertically and horizontally oriented rectangular thermal storage units," *Energy*, vol. 255, Sep. 2022, Art. no. 124521, <https://doi.org/10.1016/j.energy.2022.124521>.
- [6] C. Zhao, J. Wang, Y. Sun, S. He, and K. Hooman, "Fin design optimization to enhance PCM melting rate inside a rectangular enclosure," *Applied Energy*, vol. 321, Sep. 2022, Art. no. 119368, <https://doi.org/10.1016/j.apenergy.2022.119368>.
- [7] Y. Hong, Y. Shi, D. Bai, F. Jiao, and J. Du, "Numerical study of phase change material partitioned cavities coupled with fins for thermal management of photovoltaic cells," *Case Studies in Thermal Engineering*, vol. 56, Apr. 2024, Art. no. 104200, <https://doi.org/10.1016/j.csite.2024.104200>.
- [8] L.-L. Tian, X. Liu, S. Chen, and Z.-G. Shen, "Effect of fin material on PCM melting in a rectangular enclosure," *Applied Thermal Engineering*, vol. 167, Feb. 2020, Art. no. 114764, <https://doi.org/10.1016/j.applthermaleng.2019.114764>.
- [9] B. Fekadu and M. Assaye, "Enhancement of phase change materials melting performance in a rectangular enclosure under different inclination angle of fins," *Case Studies in Thermal Engineering*, vol. 25, Jun. 2021, Art. no. 100968, <https://doi.org/10.1016/j.csite.2021.100968>.
- [10] M. Shafiq Shahid and M. Khan Mahabat, "Effects of fin length distribution functions and enclosure aspect ratio on latent thermal energy storage performance of dual-wall-heated unit," *Journal of Energy Storage*, vol. 53, Sep. 2022, Art. no. 105247, <https://doi.org/10.1016/j.est.2022.105247>.
- [11] Ç. Yıldız, M. Arıcı, S. Nižetić, and A. Shahsavari, "Numerical investigation of natural convection behavior of molten PCM in an enclosure having rectangular and tree-like branching fins," *Energy*, vol. 207, Sep. 2020, Art. no. 118223, <https://doi.org/10.1016/j.energy.2020.118223>.
- [12] T. Mills, K. Venkateshwar, S. Tasnim Humaira, and S. Mahmud, "Numerical and experimental investigation of the melting of a PCM in an enclosure having a tree-shaped internal fin," *Thermal Science and Engineering Progress*, vol. 48, Feb. 2024, Art. no. 102434, <https://doi.org/10.1016/j.tsep.2024.102434>.
- [13] C. Zhao *et al.*, "Review of analytical studies of melting rate enhancement with fin and/or foam inserts," *Applied Thermal Engineering*, vol. 207, May 2022, Art. no. 118154, <https://doi.org/10.1016/j.applthermaleng.2022.118154>.
- [14] M. A. Aichouni, N. F. Alshammari, N. B. Khedher, and M. Aichouni, "Experimental Evaluation of Nano-Enhanced Phase Change Materials in a Finned Storage Unit," *Engineering, Technology & Applied Science Research*, vol. 10, no. 3, pp. 5814–5818, Jun. 2020, <https://doi.org/10.48084/etasr.3616>.
- [15] W.-B. Ye, "Thermal and hydraulic performance of natural convection in a rectangular storage cavity," *Applied Thermal Engineering*, vol. 93, pp. 1114–1123, Jan. 2016, <https://doi.org/10.1016/j.applthermaleng.2015.10.083>.
- [16] A. Laouer, K. Al-Farhany, M. F. Al-Dawody, and A. Hashem Liaq, "A numerical study of phase change material melting enhancement in a horizontal rectangular enclosure with vertical triple fins," *International Communications in Heat and Mass Transfer*, vol. 137, Oct. 2022, Art. no. 106223, <https://doi.org/10.1016/j.icheatmasstransfer.2022.106223>.
- [17] B. Huang, S. Yang, X. Li, J. Wang, and P. Lund D., "Strengthening of melting-solidification process in latent heat storage through sine wave shaped fins," *Journal of Energy Storage*, vol. 66, Aug. 2023, Art. no. 107494, <https://doi.org/10.1016/j.est.2023.107494>.
- [18] R. Farsani Yadollahi, A. Mahmoudi, and M. Jahangiri, "How a conductive baffle improves melting characteristic and heat transfer in a rectangular cavity filled with gallium," *Thermal Science and Engineering Progress*, vol. 16, May 2020, Art. no. 100453, <https://doi.org/10.1016/j.tsep.2019.100453>.
- [19] B. Kamkari, H. Shokouhmand, and F. Bruno, "Experimental investigation of the effect of inclination angle on convection-driven melting of phase change material in a rectangular enclosure," *International Journal of Heat and Mass Transfer*, vol. 72, pp. 186–200, May 2014, <https://doi.org/10.1016/j.ijheatmasstransfer.2014.01.014>.